

Grid Power Peak Shaving and Valley Filling Using Vehicle-to-Grid Systems

Zhenpo Wang, *Member, IEEE*, and Shuo Wang

Abstract—A strategy for grid power peak shaving and valley filling using vehicle-to-grid systems (V2G) is proposed. The architecture of the V2G systems and the logical relationship between their sub-systems are described. An objective function of V2G peak-shaving control is proposed and the main constraints are formulated. The influences of the number of connected EVs and the average value of the target curve are analyzed. The rms and the standard deviation of the difference between the target and planned curves are proposed as indices for measuring the degree of matching between the two curves. The simulation results demonstrate that peaking shaving using V2G can be effective and controllable, and the proposed control algorithm is feasible.

Index Terms—Control strategy, electric vehicle, peak shaving, smart grid, valley filling, vehicle to grid.

I. INTRODUCTION

ENVIRONMENTAL pollution and energy shortages have made electric vehicles (EV) with low noise, zero emission, and high efficiency an inevitable choice for vehicular sustainable development. In addition to the aforementioned advantages, EVs have the potential to provide other benefits within smart grids as part of a vehicle-to-grid (V2G) system [1]–[3]. V2G can help improve the reliability and stability of the grid, alleviate power shortages, reduce air pollution, and improve overall system efficiency [4]–[6]. For example, they can play an important role in helping to balance supply and demand by valley filling and peak shaving. The EV battery pack can be charged at night during low demand. The stored power can be fed power back into the grid during high-demand periods, thus helping to stabilize the grid's voltage and frequency, and providing a spinning reserve to meet sudden power demand changes. V2G may also be used to buffer renewable energy sources, such as wind turbine generators, by storing excess energy produced during windy periods, and feeding it back into the grid during high-load periods, thus effectively stabilizing the intermittency of wind power [7]–[13].

Traditionally, the electrical system infrastructure is designed to meet the highest level of demand; therefore, the system during

Manuscript received November 15, 2012; revised March 04, 2013 and April 12, 2013; accepted May 17, 2013. Date of publication June 11, 2013; date of current version June 20, 2013. This work was supported by National Natural Science Foundation of China. Paper no. TPWRD-01234-2012.

The authors are with the National Engineering Laboratory for Electric Vehicles, Beijing Institute of Technology, Beijing 100081, China (e-mail: wangzhenpo@bit.edu.cn; skywshuo@126.com).

Color versions of one or more of the figures in this paper are available online at <http://ieeexplore.ieee.org>.

Digital Object Identifier 10.1109/TPWRD.2013.2264497

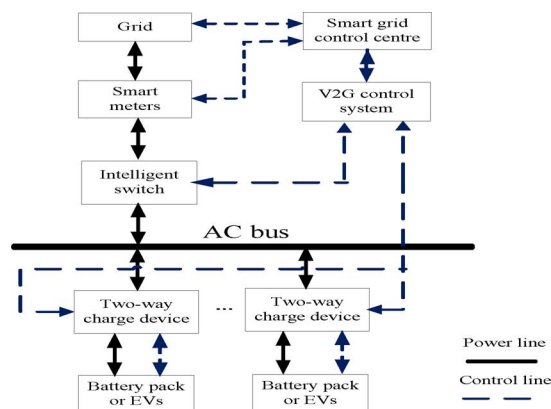


Fig. 1. V2G topology in the power-supply system.

off-peak periods is typically underutilized [14]. But in large industrial cities, the demand peak-valley gap can be as high as 40%–50% [15], [16], and peak shaving and valley filling are necessary to reduce the cost of system infrastructure and improve its utilization. Compared with other peak-shaving and valley-filling methods, V2G can be a more economical and effective solution, with the added advantage of rapid response to the grid-demand variations.

This paper proposes a V2G control algorithm for peak shaving and valley filling, taking into account vehicle requirements and load demands and considering EV and V2G constraints. An objective function of V2G peak-shaving and valley-filling control is proposed and the main constraints are formulated. The influences of the number of connected EVs and the average value of the target curve are analyzed using computer simulations.

II. PEAK SHAVING AND VALLEY FILLING USING V2G

A. General Control Strategy of V2G

Fig. 1 shows a block diagram of a V2G system. Power is measured using a smart meter. Bidirectional charge/discharge devices, connected in parallel to the ac bus, are used for energy conversion. During power transmission, the data, which include EV charging time, charging capacity, power demand, and EV number connected with the grid and so on, are exchanged within each part of the V2G system. It allows EVs to charge with demand on one hand; some of the connected EVs can also feed-back electricity to the grid in power peak on the other hand. The energy flow is multifunctional, multidirectional, and time-varying. The smart meter can calculate the kilowatt-hours of charge and discharge of every EV. The EV owners and the operators of the grid can settle accounts according to the values. Therefore, the

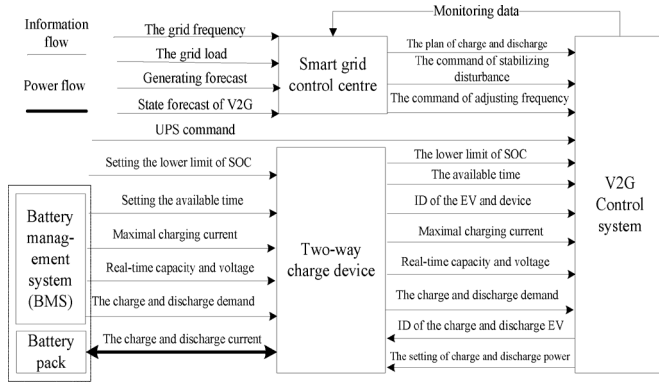


Fig. 2. Logical relationship of V2G information.

EVs not only can be the power consumer, but they can also be the supplier under this mode. The price of charge and discharge in the different period of the entire day can become the effective measure for shaving peak and filling valley.

The information exchange in a V2G system is complicated and Fig. 2 shows the logic of the data exchange. The bidirectional charge/discharge devices integrate the information of the connected EVs and then give it to the V2G control system. All of the data are sent to the smart-grid control center. The smart-grid control center issues commands to the V2G control system based on the principle of optimal energy distribution, and then the V2G control system sets the charge or discharge power command of every bidirectional charge/discharge device according to the states of the connected EVs and the general charge and discharge demand [17], [18]. The grid can also send commands to the V2G control system directly in an emergency, for example, the connected EVs are requested to work as an uninterrupted power supply (UPS).

B. Objective Function

In a V2G system, the energy storage resources used for peak shaving and valley filling are aggregated from numerous EV battery packs connected with the grid randomly. It is a time-variant random and complicated system [19], [20]. The V2G control system can predict the general available capacity and charging demand in real time according to the parameters of the connected EVs, and the smart-grid control center can determine the charge and discharge targets according to the load demand and data on available V2G capacity.

The forecast load curve can be established using statistical analysis of historical data, extrapolation methods, time-series method, Gray theory method, or artificial-neural-network methods [21]–[23]. In this paper, we assume that the forecast load curve is known. An optimal target load curve (i.e., a desired load curve incorporating peak shaving) can be obtained based on a grid configuration in a certain operation cycle. When the forecast load curve and the target load curve are known, a maximum-likelihood strategy is applied to produce a peak-shaving V2G plan. That is to say, the load curve incorporating V2G peaks shaving is close to the target load curve. To serve EVs within the V2G system and improve the load curve,

the key step is to determine the EV's available time and power. Therefore, an objective function is established as

$$\min(F) = \sum |z_i(t) - [x_i(t) + y_i(t)]| \quad (1)$$

where t is time; i is the number of a V2G service area; $x_i(t)$ is the forecast load value, determined from historical power usage; $z_i(t)$ is the target load value, derived from the states of load and vehicles; and $y_i(t)$ is the available power for peak available from the V2G system, which is determined by the available vehicles involved in the V2G and their available battery capacity.

C. Constraints

A V2G system is fundamentally different from other devices used for peak shaving and valley filling in that it relies on batteries. Battery life is influenced by the depth of discharged, number of cycles, and charge/discharge rates among other factors. Consumers usually require the batteries to be fully charged in the shortest period of time as possible to increase the vehicle's autonomy. Both battery life and charging time are therefore major constraints in a V2G system. The maximum time for recharging a battery should be set as a tradeoff between the need of having a quick recharge as desired by the consumer, and participating in peak shaving as desired by the owners of the charge station and the grid. One could envisage incentive schemes that encourage consumers to allow the participation of their vehicles in the V2G system. The V2G system could also include a prioritizing system that considers the history of the battery usage, based on data recorded by the battery-management system for example, and set an appropriate charging time.

In addition to battery and consumer constraints, the peak-shaving and valley-filling V2G system needs to comply with the following constraints:

- 1) Constraints on the power of EVs involved in the V2G system which can be expressed as follows:

$$\begin{cases} |y_i(t)| \leq a_i & a_i > 0 \\ |y_i(t)| \leq |b_i| & b_i < 0 \\ |y_i(t)| \leq |z_i(t) - x_i(t)| \end{cases} \quad (2)$$

where a_i is a positive number equal to the maximum value of the total charge power from the grid to the connected EVs, and b_i is a negative value equal to the maximum value of the total discharge power from the EVs connected to the grid.

The aforementioned constraint limits the value of $y_i(t)$ to be less than the maximum service capability of EVs, which is affected by traffic demand, and load power in area i . Meanwhile, the value of $y_i(t)$ cannot be more than the supply and demand of the grid.

- 2) Constraints on two-way current and power for each EV are represented as follows:

$$\begin{cases} 0 \leq C_{ij}^c \leq C_{cm} \\ 0 \leq C_{ij}^d \leq C_{dm} \\ -I_{cm} \times V_{ij}^c \leq P_{ij} \leq I_{dm} \times V_{ij}^d \end{cases} \quad (3)$$

where j is the vehicle's code, C_{ij}^c is the charge ratio, C_{ij}^d is the discharge ratio, C_{cm} is the available maximum charge ratio, C_{dm} is the available maximum discharge ratio, V_{ij}^c is the charge voltage, V_{ij}^d is the discharge voltage, I_{cm} is the charge current within the maximum charge ratio, C_{cm} , I_{dm} is the current within the maximum discharge ratio C_{dm} , and P_{ij} is the available power of the EV.

The current and power of each connected EV are limited by the battery pack. The maximum charge and discharge current cannot be more than the charge current I_{cm} and the discharge current I_{dm} . Besides the current, the power limit relies on the voltage of the EV battery pack under this charge and discharge current.

- 3) The constraints on the capacity for each EV battery pack are

$$\begin{cases} \Delta Q_{ij}^{\max} = (\text{SOC}_{\max} - \text{SOC}_{\min})Q_e \\ 0 \leq \Delta Q_{ij}^c \leq (\text{SOC}_{\max} - \text{SOC}_{ij})Q_e \\ 0 \leq \Delta Q_{ij}^d \leq (\text{SOC}_{ij} - \text{SOC}_{\min})Q_e \end{cases} \quad (4)$$

where SOC_{ij} is the real-time capacity state, SOC_{\max} is the maximum value of SOC, SOC_{\min} is the minimum value of SOC. ΔQ_{ij}^{\max} is the maximum available capacity of the battery pack, ΔQ_{ij}^c is the available charge capacity in SOC_{ij} , ΔQ_{ij}^d is the available discharge capacity in SOC_{ij} , and Q_e is the rated capacity of the EV battery pack.

To ensure the battery pack's life and energy efficiency, the range of SOC is limited. The maximum available capacity is decided by the rated capacity and the difference between SOC_{\max} and SOC_{\min} . In the state of SOC_{ij} , the available charge or discharge capacity is limited by the second or the third expression in (4), respectively.

- 4) EV user-setting constraints are also important factors that affect the capability of V2G peak shaving. For transportation, EV should satisfy the driving demand first, which means the EV user may set the upper and lower limits of SOC and the special period in which the EV can be involved in V2G system. The EV user set parameters can be represented as follows:

$$\text{SOC}'_{\min} \leq \text{SOC}'_{ij} \leq \text{SOC}'_{\max} \quad (5)$$

where SOC'_{\min} and SOC'_{\max} are the lower and upper limits of SOC set by the user, respectively. To ensure the safety and life of the EV battery pack, SOC'_{\min} cannot be lower than SOC_{\min} , and the SOC'_{\max} cannot be higher than SOC_{\max} . When the EV is connected to the grid, the state of EV is decided by these constraints. If SOC_{ij} is lower than SOC'_{\min} , the EV needs to be preferably in the charge state. If SOC_{ij} is higher than SOC'_{\max} , then the EV can enter into the discharge state. If SOC_{ij} is between SOC'_{\min} and SOC'_{\max} , the EV operating state is decided by the V2G control system according to the requirements of the V2G system.

The user may set up the charging time and period, during which EV can be involved in the V2G service according to his or her own demand. But besides the constraints of the

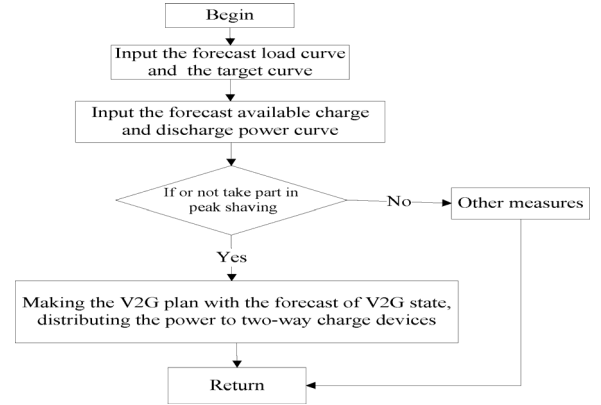


Fig. 3. Decision-making process of the V2G control system.

EV's application requirement, the user may also be influenced by electricity tariffs during the day

$$\begin{aligned} t &\geq T_b \\ T_{vb} &\leq t \leq T_{ve} \end{aligned} \quad (6)$$

where T_b is the start set point for charging, and the charging time is usually unlimited before SOC reaches the maximum value, and T_{vb} and T_{ve} are the start and end set point for EVs to be involved in the V2G system.

D. Peak-Shaving Control Process

The V2G control system makes a plan on the basis of the daily target load and the states of the connected EVs. The final result is a V2G plan curve, and the objective of peak-shaving control is to match the plan curve to the target curve within the limits of error, using the bidirectional charge/discharge devices to distribute the load power according to the constraints mentioned before. Fig. 3 illustrates the general control and decision-making process. Initially, the input is the forecast grid load curve, the target curve, and the forecast-available charge and discharge power curve of the connected EVs. When the grid requires the power peak to be shaved and the connected EVs are able to provide enough power, the process of peak shaving and valley filling can be started by the V2G system. Otherwise, other measures will need to be used to control the supply and load.

Fig. 4 shows the realization of the detailed V2G plan curve. The forecast load curve and the target load curve are assumed to be known. The output result, the V2G plan curve, is acquired through the smart-grid control center and the V2G control system. The constraints mentioned before, such as EV number, the device's state, battery pack's capacity, and so on, have to be considered.

As shown in Fig. 4, the solution for the V2G plan curve begins from the judgment of the charge or discharge state of the battery.

- 1) Consider the case of $x_i(t) - z_i(t) > 0$, at time T_0 when the vehicles are in the discharge state. If $|x_i(t) - z_i(t)| < |b_i|$, which means that the grid demand is less than V2G-available maximum discharge power, the actual discharge power is $y_i(t) = |x_i(t) - z_i(t)|$, which is equal to the actual grid demand. If $x_i(t) - z_i(t) \geq |b_i|$, which means the grid

TABLE I
EV PARAMETERS IN THE V2G SYSTEM

Serial	Type	Numbers	Rated capacity/Ah	Rated voltage/V	Max discharge power/kW	Maximum charge power/kW
1	Passenger car	2000	80	320	32.8	18.5
2	Municipal trucks	600	200	384	82.2	51.1
3	Public traffic vehicle	1000	360	384	147.9	108.0

TABLE II
EV-AVAILABLE POWER IN V2G WITH THE DIFFERENT TIMES (UNIT: MEGAWATTS)

Type	Passenger car		Municipal truck		Public traffic vehicle		Total	
	Charge proportion/ power	Discharge proportion/ power	Charge proportion/ power	Discharge proportion/ power	Charge proportion/ power	Discharge proportion/ power	Charge power	Discharge power
0:00-6:00	95%/ 62.44	/	20%/ 9.86	/	98%/ 144.93	/	217.23	/
6:00-8:00	10%/ 6.57	10%/ 6.57	90%/ 44.37	70%/ 34.51	5%/ 7.40	5%/ 7.40	58.33	48.47
8:00-17:00	90%/ 59.16	90%/ 59.16	90%/ 44.37	70%/ 34.51	40%/ 59.16	40%/ 59.16	162.66	152.82
17:00-19:00	10%/ 6.57	10%/ 6.57	90%/ 44.37	70%/ 34.51	5%/ 7.39	5%/ 7.39	58.33	48.47
19:00-24:00	95%/ 62.44	/	20%/ 9.86	/	98%/ 144.93	/	217.2	/

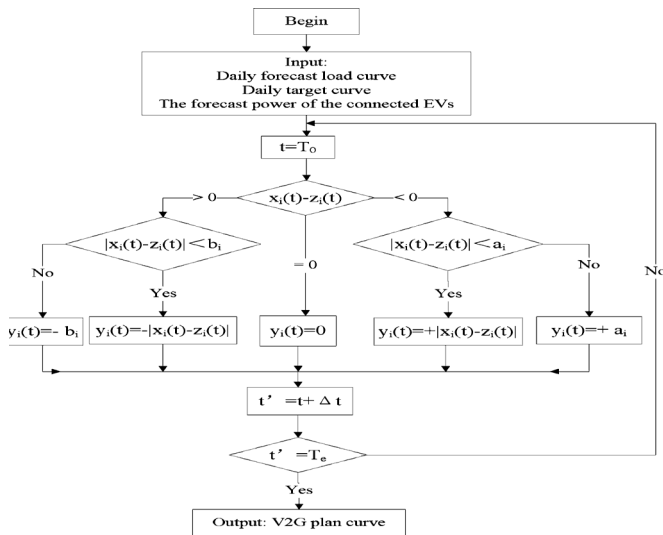


Fig. 4. Process of determining the V2G plan curve.

discharge demand is greater than or equal to V2G-available maximum discharge power, the actual discharge power is $y_i(t) = b_i$, that is, the maximum value of available power from the EVs within the V2G system.

- 2) Consider the case of $x_i(t) - z_i(t) < 0$, at time T_0 , when the vehicles are in the charging state. If $|x_i(t) - z_i(t)| < a_i$, which means the charge demand of EVs is less than the grid available maximum charge power, the charge power is then $y_i(t) = |x_i(t) - z_i(t)|$, which is equal to the actual power demand of EVs. If $|x_i(t) - z_i(t)| \geq a_i$, which means the charge demand of EVs is greater than or equal to the grid available maximum charge power, the charge power is $y_i(t) = a_i$, which is the maximum charge power from the grid. In this condition, EVs begin to charge, in turn, according to the priority of connecting to the grid.

- 3) When $x_i(t) - z_i(t) = 0$, there is no energy exchange between the grid and EVs at T_0 in area i , which means $y_i(t) = 0$.

When the calculation is finished at T_0 , Δt is added T_0 and the calculations are repeated for the next time step, if the end of the V2G peak-shaving and valley-filling operation has not been reached. The V2G planning curve can be exported in real time.

III. DEVELOPMENT OF THE SIMULATION SYSTEM

A. Solution Process of the V2G Plan Curve

Since there are no available test sites of V2G systems, the algorithm just shown is tested using simulations. The numbers of all kinds of vehicles are scaled down on the basis of the average proportions based on data available in some cities [21], [24], [25]. The vehicles are assumed to be pure electric vehicles, and not including plug-in hybrid electric vehicles as assumed in most references [1], [5], [9], [8], [13], [18]. It is assumed that 5% of all passenger cars are electric vehicles. Municipal vehicles, such as sanitation trucks and logistics vehicles, and public traffic vehicles are all assumed to be EVs. The EV parameters are shown in Table I.

With regards to the distribution of operation times, public traffic vehicles are assumed to mainly operate in the daytime. Municipal trucks are assumed to operate mostly at night, and the passenger cars are assumed to be used mainly during day working hours, particularly during the rush hours. The maximum V2G-available power can be estimated on the basis of the EV operation demands and the EV battery pack capacity as shown in Table II.

In Table II the charging proportion is the proportion of the parked and charging EVs at specific times, and the discharging proportion is the proportion of EV that can feed power into the grid. The proportion values are estimated from data parking proportion in specific areas [21], [24], [25], taking into account EV grid characteristics. For example, some EVs can feed power into the grid at night, but at this time, the grid is in the valley time

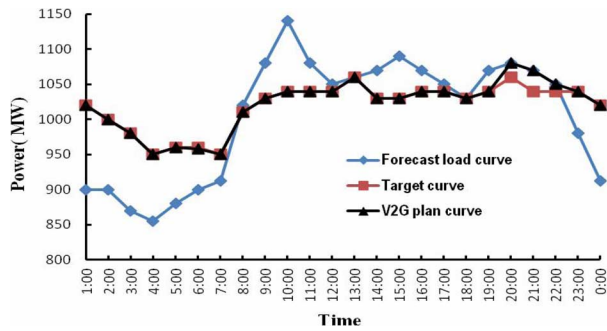


Fig. 5. Comparison of the power load before and after peak shaving.

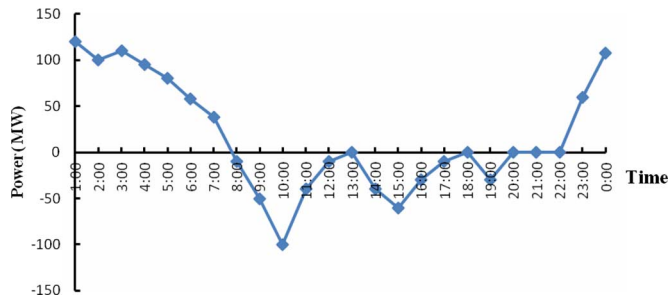


Fig. 6. Power distribution of EVs in V2G.

and does not need the power. Power flows between EVs through the grid are not considered in this paper.

The forecast load curve in this paper was scaled down according to the urban power load in one day. The time distribution and trend obey the practical load curve, and the target curve is designed with the consideration of the grid efficiency, EV operation and its power, and the time-of-use power, etc. [15], [16]. The two curves are shown in Fig. 5. The valley-filling demand is about 23:00 P.M. to 7:00 A.M. The maximum peak-shaving value is about 10% of the general power load at 10:00 A.M.

The charge and discharge power of the connected EVs was simulated using Matlab according to the control process described in Fig. 3 and aforementioned constraints and assumed conditions. As an example, the output value at 1:00 is analyzed as follows. The forecast load value ($x_i(t), t = 1 : 00$) is obviously less than the target load value ($z_i(t), t = 1 : 00$). That is to say, the grid is in the valley time and its spare power can charge the EVs. The absolute value of the difference between the $x_i(1 : 00)$ and $z_i(1 : 00)$ is 120 MW, which is the max power value of the grid supply. At the same time, the max charging demand is 217.23 MW as shown in Table II. According to the control process and the first boundary condition in 2.3, the charging power should be limited to 120 MW. The target value and the V2G plan value are the same in this time too. The other boundary conditions are mainly about how to distribute the power in different EVs.

The total output is shown in Fig. 6 where positive power means charging and the negative value means discharging. Valley filling mainly occurs at 23:00 P.M. to 7:00 A.M. and peak shaving occurs between 8:00 A.M. to 12:00 A.M. and 14:00 P.M. to 16:00 P.M. The maximum shaved power is more than 100 MW, which is approximate 9% of the maximum power load.

TABLE III
COMPARISON OF THE PEAK AND VALLEY POWER VALUES BEFORE AND AFTER SHAVING

Subject	Before peak shaving	Target value	After peak shaving
Peak value(MW), P_p	1090	1060	1080
Valley value(MW), P_v	855	950	950
Peak and valley difference(MW), P_d	235	110	130
Proportion (%): P_d/P_p	21.56	10.38	12.04
Proportion (%): P_d/P_v	27.49	11.58	13.68

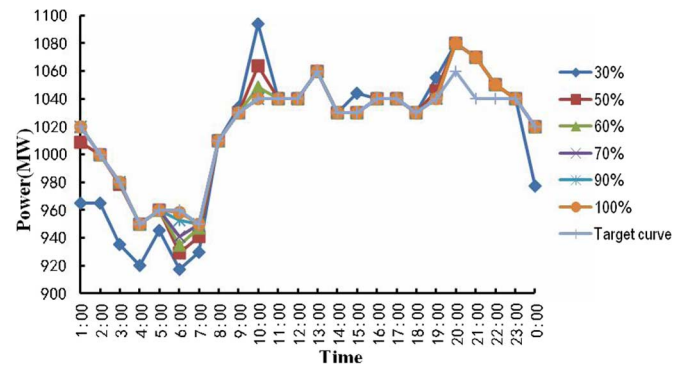


Fig. 7. Effect of the number of connected EVs on peak shaving and valley filling.

Fig. 5 also shows a comparison between the target curve and the V2G plan curve. It can be seen that the V2G plan curve is close to the target curve. The obvious difference occurs between 19:00 P.M. to 21:00 P.M. because of the small number of connected EVs. The period of the peak value shifts from morning at 10:00 to evening at 20:00 according to the V2G plan curve. Table III shows a comparison between the characteristic values before and after the peak shaving. In general, the peak value decreases 10 MW, and the valley value increases 95 MW. The difference between the peak and valley is obviously reduced, and the value of peak-valley gap is decreased by about 50%.

B. Effect of EV Numbers on Peak Shaving

The aforementioned simulations were carried out on the basis of the maximum number of connected EVs and the maximum-available powers. However, the vehicles connect to the grid randomly and the available power is not constant. Therefore, the total available power of the V2G may be smaller than the presumed one, which affects the peak-shaving results. More simulations were therefore carried out for such conditions that 90%, 70%, 60%, 50% and 30% of these vehicles are available to participate in V2G. The results are shown in Fig. 7. Table IV compares achievable power for different numbers of connected vehicles with the target value at 6:00 A.M. and 10:00 A.M. The fewer the number of available EVs, the greater the difference between

TABLE IV
EFFECT OF EV NUMBERS ON PEAK SHAVING AT 6:00 A.M. AND 10:00 A.M. (IN MEGAWATTS)

Time	Target value	100%	90%	70%	60%	50%	30%
6:00AM	960	958.3	952.5	940.8	935	929.2	917.5
10:00AM	1040	1040	1040	1040	1048.3	1063.6	1094.2

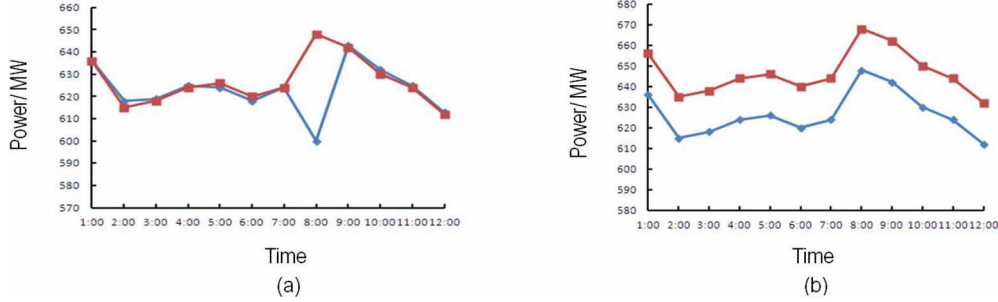


Fig. 8. (a) Effect of extreme value in the curve. (b) Effect of the similar but parallel curve.

the target curve and the achievable load curve, especially during the peak and valley periods, as expected.

The rms and the standard deviation of the difference between the target curve and the V2G plan curve are calculated using the following formulae:

$$D_p = \sqrt{\frac{\sum_{t=1}^{24} h_i(t)^2}{24}} \quad (7)$$

$$A_p = \sqrt{\frac{\sum_{t=1}^{24} [h_i(t) - \bar{h}_i]^2}{24}} \quad (8)$$

where $h_i(t)$ is the difference between the target curve and the V2G plan curve at time i , that is, $h_i(t) = y_i(t) - z_i(t)$, \bar{h}_i is the mean value of $h_i(t)$, that is, $\bar{h}_i = \sum_{t=1}^{24} h_i(t)/24$.

The difference in square root cannot detect extreme values of $h_i(t)$, and the standard deviation cannot detect similar but parallel curves as illustrated. Examples of these special cases are shown in Fig. 8.

The rms and the standard deviation for different EV numbers are shown in Table V. It shows that the two evaluation indices are increased along with the decrease of EV numbers. The changes of the two indices are small when the connected EVs are more than 70%. However, the two indices increase significantly when the EV numbers are less than 70%. It also shows that the corresponding values of the two evaluation indices are very close, which illustrates that the two special cases in Fig. 8 did not occur.

C. Effect of the Target Curve on Peak Shaving

Assuming that the number of EVs is constant, simulation results assuming different target curves are shown in Fig. 9. The target powers are 60%, 80%, 90%, 100%, 110%, 120%, and 140% of the original values of the target curve from bottom to top, respectively. The rms and the standard deviation of the difference between the target and plan curves are shown in

TABLE V
RMS AND STANDARD DEVIATION OF THE DIFFERENCE BETWEEN THE PLANNED AND TARGET CURVES FOR EV NUMBERS

The proportion of the EVs	The difference square root	The standard deviation
30%	25.98	25.50
50%	11.46	11.53
60%	9.36	9.36
70%	8.58	8.58
80%	7.79	7.80
100%	7.65	7.66

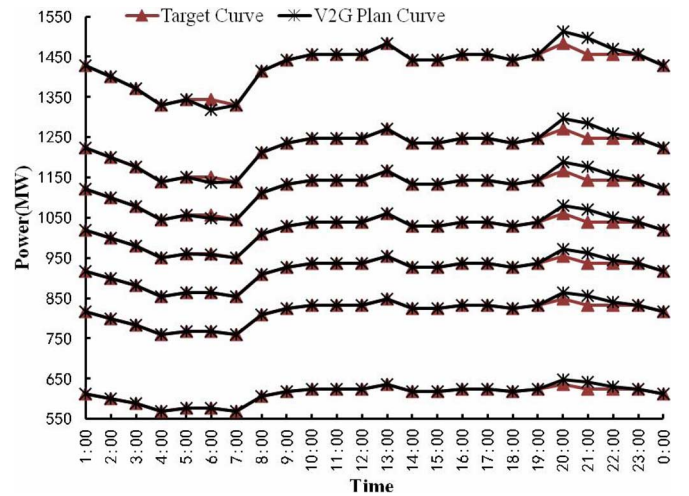


Fig. 9. Simulation results for different target curves.

Table VI. It is clear that the capability of peak shaving increases with the decrease in power of the target curve.

D. Technical Implementation Methods for Peak Shaving

In accordance with the influencing factors analyzed before, it is unrealistic to increase the capacity of power supply by controlling the number of EVs connected to the grid, and it is also

TABLE VI
CALCULATION RESULTS OF THE TWO ROOTS IN DIFFERENT TARGET CURVES
(*THE PERCENTAGE IS THE SPECIFIC VALUE OF THE POWER TO
THE ORIGINAL TARGET CURVE)

The percentage*	The difference square root	The standard deviation
60%	4.58	4.59
80%	6.11	6.12
90%	6.87	6.89
100%	7.65	7.66
110%	8.55	8.58
120%	9.58	9.6
140%	11.91	11.92

unpractical to improve the forecast load curve by controlling the electricity using time. These two aspects can be realized by macroincentive policies of the electric power system, for example, by increasing the electricity using price and EV electric-supply price during the peak period, cutting down the EV electric supply price during the valley period.

An important reason why EV users are not willing to connect EVs to the network is that the grid lacks a real-time energy supply and demand information, and the EV users have no acquaintance with the accurate onboard energy. Combining the V2G control strategy and information-exchange analysis in Part II, the prediction ability of EV onboard energy and driving mileage should be improved from a technical point of view. The communication between the EVs and wireless terminals (smart phone, Ipad, etc.) should be achieved through the wireless networks (GPRS, 3G, etc.), so that EV users will be well informed of onboard energy info and informed of electricity supply and demand info of the grid. Users will also be able to set and revise the time when EV connects to the grid, the time when EV is charged by the grid, the time when EV supports electricity to the grid, and some parameters like power through smart phones or some other devices. After all of the functions mentioned before are achieved, the target that EV users adjust their vehicles' onboard energy application strategy will be reached, so that the number of EVs that are willing to connect to the grid is increased, in which the power-supply capability is improved during peak hours. As shown in Fig. 5, if users are real time informed that the EV number connected to the grid is too small and the grid needs some more electric energy during 19:00–22:00, and the electricity price is very high, the standby EV users will be very happy to connect their EVs to the grid just by setting some parameters through their smart phone. Then, the goal to optimize the allocation of resources, to shift loads, and to improve the grid quality is achieved.

IV. CONCLUSION

This paper describes peak-shaving and valley-filling control using a V2G system. The functions of each module and their logical relationship are described. Aiming at matching the target power curve and the V2G plan curve, an objective function of the peak-shaving and valley-filling control is proposed. The corresponding constraints on the connected EV numbers, the characteristics of the EV battery packs, and the user set parameters are analyzed and formulated, and the peak-shaving and valley-filling control flow and logic operations are established.

A simulation system is developed based on available data for typical cities. The influences of the number of connected EVs and the target curve are analyzed quantitatively. With the increase of connected EVs' number or the decrease of the average target, the V2G plan curve becomes closer to the target curve, and the effectiveness of peak shaving and valley filling using the V2G system is increased. Considering the randomness of the connected EV numbers, the V2G system should be designed with redundant EV numbers in order to ensure the reliability of the V2G system.

The rms and the standard deviation, of the difference between the target and planned curves, are proposed as two evaluation indices for the degree of matching between the target curve and the V2G plan curve. The smaller the values of the two evaluation indices, the better the matching between the two curves. The simulation results suggest that good matching is achieved when the two indices are both under 10. The simulation results demonstrate that the V2G peak-shaving and valley-filling control strategy and its constraints are reasonable and effective. If the EV number is large enough in the area, the V2G system can replace other peak-shaving and valley-filling methods completely.

ACKNOWLEDGMENT

The authors would like to thank Dr. S. M. Sharkh, of the University of Southampton, and Dr. C. Ke of the Beijing Institute of Technology, for discussions and critical reading of the manuscript. The project (No. 61004092) was about the optimal control of the V2G system.

REFERENCES

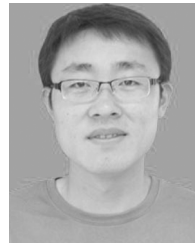
- [1] B. K. Sovacool and R. F. Hirsh, "Beyond batteries: An examination of the benefits and barriers to plug-in hybrid electric vehicles (PHEVs) and a vehicle-to-grid (V2G) transition," *Energy Policy*, vol. 37, pp. 10095–11003, 2009.
- [2] H. Turton and F. Moura, "Vehicle-to-grid systems for sustainable development: An integrated energy analysis," *Technol. Forecast. Social Change*, vol. 75, pp. 1091–1108, 2008.
- [3] Y. Saber and G. K. Venayagamoorthy, "Intelligent unit commitment with vehicle-to-grid—A cost-emission optimization," *J. Power Sources*, vol. 195, pp. 898–911, 2010.
- [4] K. Kempton and J. Tomic, "Vehicle-to-grid power implementation: From stabilizing the grid to supporting large-scale renewable energy," *J. Power Sources*, vol. 144, pp. 280–294, 2005.
- [5] W. Kempton and S. E. Letendre, "Electric vehicles as a new power source for electric utilities," *Transport. Res. D: Transport Environment*, vol. 2, pp. 157–175, 1997.
- [6] S. Han, H. Han, and K. Sezaki, "Design of an optimal aggregator for vehicle-to-grid regulation service," presented at the IEEE Power Energy Soc. Conf. Innovative Smart Grid Technol., Gaithersburg, MD, 2010.
- [7] A. K. Madawala and D. J. Thrimawithana, "A bidirectional inductive power interface for electric vehicles in V2G systems," *IEEE Trans. Ind. Electron.*, vol. 58, no. 10, pp. 4789–4796, Oct. 2011.
- [8] A. K. Srivastava, B. Annabathina, and S. Kamalasan, "The challenges and policy options for integrating plug-in hybrid electric vehicle into the electric grid," *Elect. J.*, pp. 83–91, 2010, vol. 1.
- [9] R. Sioshansi and P. Denholm, "Emissions impacts and benefits of plug-in hybrid electric vehicles and vehicle-to-grid services," *Environmental Sci. Technol.*, vol. 43, pp. 1199–1204, 2009.
- [10] W. Kempton and J. Tomic, "Vehicle-to-grid power fundamentals: Calculating capacity and net revenue," *J. Power Sources*, vol. 144, pp. 268–279, 2005.
- [11] S. Han, H. Han, and K. Sezaki, "Development of an optimal vehicle-to-grid aggregator for frequency regulation," *IEEE Trans. Smart Grid*, vol. 1, no. 1, pp. 65–72, Jun. 2010.

- [12] J. R. Pillai and B. B. Jensen, "Integration of vehicle-to-grid in the western Danish power system," *IEEE Trans. Sustain. Energy*, vol. 2, no. 1, pp. 12–19, Jan. 2011.
- [13] A. Hajimiragha, C. A. Cañizares, M. W. Fowler, and A. Elkamel, "Optimal transition to plug-in hybrid electric vehicles in Ontario, Canada, considering the electricity-grid limitations," *IEEE Trans. Ind. Electron.*, vol. 57, no. 2, pp. 690–701, Feb. 2010.
- [14] International Energy Agency, Technology roadmap smart grids. 2011. [Online]. Available: http://www.iea.org/publications/publications/publication/smartgrids_roadmap.pdf
- [15] X. Bai, K. Clark, G. A. Jordan, N. W. Miller, and R. J. Piwko, "Intermittency Analysis Project: Appendix B, Impact of intermittent generation on operation of California Power Grid." 2007. [Online]. Available: <http://www.uwig.org/CEC-500-2007-081-apb.pdf>
- [16] International Energy Agency, Prospects for large-scale energy storage in decarbonised power grids. [Online]. Available: http://www.iea.org/publications/publications/publication/energy_storage.pdf
- [17] X. Wang, P. Yan, and L. Yang, "A V2G vector control model of electric car charging and discharging machine," presented at the Int. Conf. Advanced Mechatronic Systems-Final Program, Zhengzhou, China, 2011.
- [18] S. Han, H. Han, and K. Sezaki, "Estimation of achievable power capacity from plug-in electric vehicles for V2G frequency regulation: Case studies for market participation," *IEEE Trans. Smart Grid*, vol. 2, no. 4, pp. 632–641, Dec. 2011.
- [19] C. Quinn, D. Zimmerle, and T. H. Bradley, "The effect of communication architecture on the availability, reliability, and economics of plug-in hybrid electric vehicle-to-grid ancillary services," *J. Power Sources*, vol. 195, pp. 1500–1509, 2010.
- [20] Z. Yang, S. Yu, W. Lou, and C. Liu, "Privacy-preserving communication and precise reward architecture for V2G networks in smart grid," *IEEE Trans. Smart Grid*, vol. 2, no. 4, pp. 697–706, Dec. 2011.
- [21] Y. Rui, "Research on the mathematical method and its application in electric load forecast," Ph.D. dissertation, Dept. Mech. Elect. Eng., Central South University, Hunan, China, 2006.
- [22] K. Cui, J. R. Li, W. Chen, and H. Y. Zhang, "Research on load forecasting methods of urban power grid," *Elect. Power Technol. Econom.*, vol. 21, pp. 33–38, 2009.
- [23] G. Yao, Z. S. Chen, and X. Z. Li, "BP network based on particle swarm optimization of short-term electric load forecasting," *J. Guangdong Univ. Petrochem. Technol.*, vol. 21, pp. 47–50, 2011.
- [24] V. N. Register, "Integrated action plan to reduce vehicle emissions," May 20, 2012. [Online]. Available: http://www.adb.org/documents/others/ReduceVehicleEmissions_VIE/Reduce_Vehicle_Emissions.pdf
- [25] International Energy Agency, "CO2 emissions from fuel combustion," May 23, 2012. [Online]. Available: <http://www.iea.org/co2highlights/co2highlights.pdf>



Zhenpo Wang (M'13) received the B.S. degree in vehicle engineering from the School of Mechanical Engineering, Tongji University, Shanghai, China, in 2000 and the Ph.D. degree in vehicle engineering from the School of Mechanical Engineering, Beijing Institute of Technology, Beijing, China, in 2005.

After graduation, he was a Lecturer and an Associate Professor at the National Engineering Laboratory for Electric Vehicles, Beijing Institute of Technology, Beijing China, in 2005 and 2007, respectively. Since 2010, he has been the Deputy Director of the laboratory. His main research interests are in the areas of the distributed control system, V2G control strategy, the energy system optimization of electric vehicles, and power battery management.



Shuo Wang was born in China in 1988. He received the B.S. degree in vehicle engineering from Beijing Institute of Technology, Beijing, China, in 2010 and the M.Sc. degree in vehicle engineering from the National Engineering Laboratory for Electric Vehicles, Beijing Institute of Technology, in 2013.

His main research interests are in the areas of battery thermal management and V2G control strategy.